METHODS AND APPLICATIONS

Patterning protein complexes on DNA nanostructures using a GFP nanobody

R. F. Sommese,[1] R. F. Hariadi,[2,3] K. Kim,[1] M. Liu,[3,4] M. J. Tyska,[5] and S. Sivaramakrishnan[1]*

[1]Department of Genetics, Cell Biology, and Development, University of Minnesota, Minneapolis, Minnesota 55455
[2]Department of Physics, Arizona State University, Tempe, Arizona 85287
[3]Biodesign Center for Molecular Design and Biomimetics, Arizona State University, Tempe, Arizona 85287
[4]School of Molecular Sciences, Arizona State University, Tempe, Arizona 85287
[5]Department of Cell and Developmental Biology, Vanderbilt University Medical Center, Nashville, Tennessee 37232

Received 25 February 2016; Revised 15 August 2016; Accepted 15 August 2016
DOI: 10.1002/pro.3020
Published online 00 Month 2016 proteinscience.org

Abstract: DNA nanostructures have become an important and powerful tool for studying protein function over the last 5 years. One of the challenges, though, has been the development of universal methods for patterning protein complexes on DNA nanostructures. Herein, we present a new approach for labeling DNA nanostructures by functionalizing them with a GFP nanobody. We demonstrate the ability to precisely control protein attachment via our nanobody linker using two enzymatic model systems, namely adenylyl cyclase activity and myosin motility. Finally, we test the power of this attachment method by patterning unpurified, endogenously expressed Arp2/3 protein complex from cell lysate. By bridging DNA nanostructures with a fluorescent protein ubiquitous throughout cell and developmental biology and protein biochemistry, this approach significantly streamlines the application of DNA nanostructures as a programmable scaffold in biological studies.

Keywords: DNA nanostructures; nanobody; GFP; myosin VI; adenylyl cyclase; Arp2/3

Introduction

DNA nanotechnology provides the ability to precisely control both protein stoichiometry and geometry akin to cellular organization. Over the last few years, researchers have started to apply these strengths to questions of protein ensemble behavior[1–4] and enzyme pathway dynamics.[5,6] Further validating their use for biological applications, DNA

Additional Supporting Information may be found in the online version of this article.

Broader statement: One of the challenges of DNA nanotechnology has been the development of universal methods for patterning proteins onto nanostructures. Herein, we present a new approach for labeling DNA nanostructures with unpurified, endogenously-expressed protein complex using a GFP-nanobody. By bridging DNA nanostructures with a fluorescent protein ubiquitous throughout cell and developmental biology and protein biochemistry, this approach significantly streamlines the application of DNA nanostructures as a programmable scaffold in biological studies.

Disclosure: The authors declare no competing interests.

Grant sponsor: American Heart Association Scientist Development Grant; Grant number: 13SDG14270009; Grant sponsors: NIH Grants; Grant numbers: 1DP2 CA186752-01 and 1-R01-GM-105646-01-A1; Grant sponsor: Life Sciences Research Foundation.

*Correspondence to: Department of Genetics, Cell Biology, and Development, 4-130 MCB, 420 Washington Avenue SE, University of Minnesota, Twin Cities, Minneapolis, MN 55455. E-mail: sivaraj@umn.edu

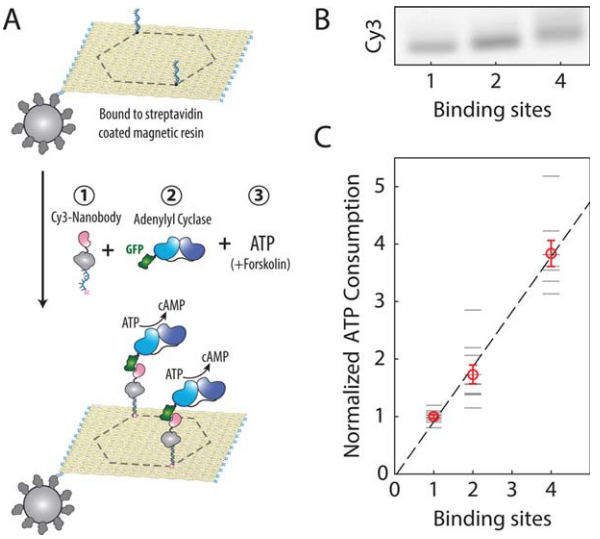

Figure 1. Chemical readout of GFP-tagged adenylyl cyclase on DNA nanostructures. (A) Schematic of activity assay measuring the stoichiometric attachment of GFP-labeled adenylyl cyclase to Cy5-labeled DNA nanostructures. Nanostructures with two binding sites are bound to magnetic resin and (1) labeled with Cy3-tagged GFP-nanobody, (2) incubated with GFP-labeled adenylyl cyclase, and (3) reacted with 100 μ*M* ATP and 100 μ*M* forskolin at 30°C. (B) Nanobody-labeled nanostructures with one, two, or four binding sites have distinct gel-shifts in 0.67% agarose 0.1% SDS gels. (C) Cy5-labeled DNA nanostructures decorated with increasing numbers of GFP-labeled adenylyl cyclase show a clear linear increase in enzymatic activity relative to attachment sites ($R^2 = 0.87$). Error bars represent ± SEM ($n > 5$).

nanostructures remain highly stable and functional in cell lysate.[7] One of the major barriers, however, has been the attachment of proteins of interest to DNA nanostructures. One method is directly cross-linking short DNA attachment oligos to the target protein.[5,6] Many proteins, though, have limited stability, and thus even mild chemical modification may lead to enzyme inactivation. Alternative methods include using a secondary attachment protein tag such as DNA aptamer binding proteins,[8] biotin–streptavidin based linkages,[9,10] unnatural amino acids,[11] or small labeling proteins such as "SNAP" or "Halo" tags.[1–4,10,12] In particular, SNAP and Halo tags have been used because they allow direct labeling of the protein of interest to specific DNA oligos and thus provide the needed specificity for multiprotein scaffolds. Limitations of these methods, though, are that proteins have to be re-engineered with the protein tags, additional purification methods are still required to remove excess label, and there is often a trade-off between labeling efficiency and protein stability. To be more widely applicable, an attachment system is needed which takes advantage of the widespread use of specific protein tags throughout the biological sciences, such as the fluorescent family of GFP proteins.

Here we present a technical advance for labeling of DNA nanostructures using a nanobody attachment strategy. Nanobodies are small (12–15 kDa), monomeric, single-domain antibodies that bind to their antigens strongly with dissociation constants in the picomolar to nanomolar range.[13] Nanobodies have been produced using a variety of expression systems to high purity and are extremely stable.[13] We used a GFP-nanobody that can recognize both GFP and YFP and has one-to-one stoichiometric binding to GFP with a $K_D < 2$ n*M*.[14,15] We test the stoichiometric control of our nanobody-based attachment system using two previously published protein assay systems: adenylyl cyclase enzymatic activity[16] and actin-based myosin VI motility.[2] Finally, we demonstrate the strength of this approach by patterning endogenously expressed yeast Arp2/3 complex on DNA nanostructures.

Results

We designed our GFP-nanobody with a SNAP tag for single-stranded, Cy3-oligo DNA labeling. We tested this nanobody using a Cy5-labeled flat rectangular DNA nanostructure (~100 nm × ~80 nm) with a biotin purification tag and 1–6 protein attachment sites[4] (Supporting Information Fig. S1). These attachment sites allow us to specifically decorate our nanostructures with Cy3-oligo labeled GFP-nanobodies, as illustrated in the 0.67% agarose 0.1% SDS gel [Fig. 1(A,B)].

We performed two distinct tests to evaluate stoichiometric binding through the GFP nanobody. We first tested our system via an enzymatic chemical reaction using adenylyl cyclase[16] (Fig. 1). Adenylyl cyclase is a key signaling enzyme in the cell which converts adenosine triphosphate (ATP) into 3′,5′-cyclic AMP (cAMP).[17] Using 0.67% agarose 0.1% SDS gels and Cy5 intensity to correct for total amount of nanostructures, we measured the forskolin-stimulated enzymatic activity of adenylyl cyclase on nanostructures bound to magnetic beads with one, two or four attachment sites. Labeled nanostructures show a clear linear increase in enzymatic activity relative to the number of attachment sites [$R^2 = 0.87$; Fig. 1(C)].

The second system we used to test our nanobody-based adaptor was the collective movement of myosin VI motor proteins on a model 2D cellular actin network [Fig. 2(A,B)]. Myosin VI is an ATP-driven molecular motor that is involved in numerous intracellular processes such as the movement and transportation of cargo and organelles throughout the cell.[18] Previous work from our group has shown that the run length for myosin-bound nanostructures on model cellular actin networks isolated from fish keratocytes increases with increasing motor number.[2] In addition to higher complexity, this assay also tests the stability of nanobody–protein

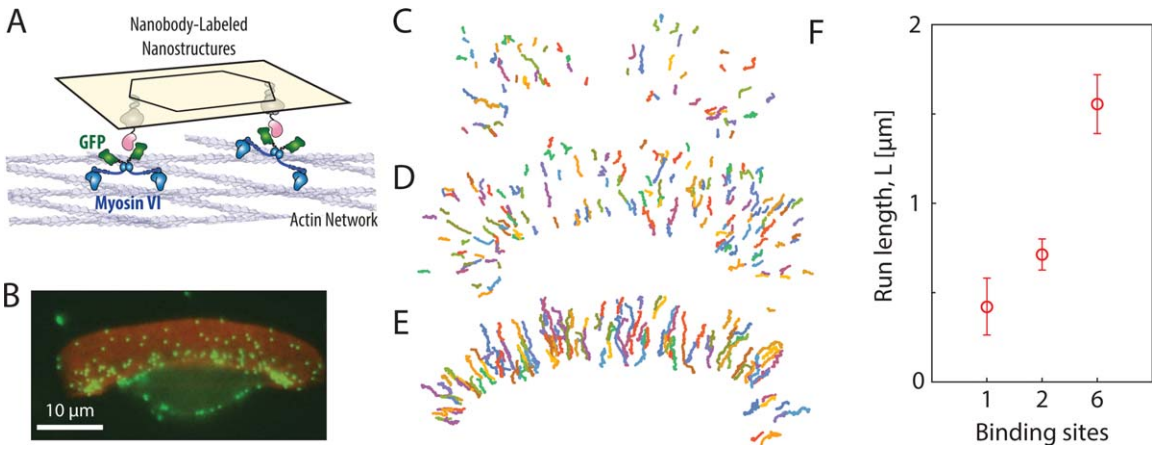

Figure 2. Mechanochemical measurement of GFP-tagged myosin VI on nanostructures. (A) Schematic of myosin VI-labeled flat rectangular DNA origami nanostructures interacting with a keratocyte-derived actin network. (B) Representative detergent-extracted keratocyte actin network with Alexa488-phalloidin labeled actin (red) and nanobody-labeled DNA nanostructures (green). (C–E) Representative trajectories of myosin VI-decorated nanostructures on the keratocyte-derived actin network labeled with (C) one, (D) two, or (E) six nanobody adaptors at 2 m*M* ATP. (F) Mean run length as a function of nanostructure binding sites. Error bars represent ± SEM ($n > 800$ trajectories).

interaction under cyclic mechanical forces. We used nanostructures with one [Fig. 2(C)], two [Fig. 2(D)], and six [Fig. 2(E)] attachment sites. Indeed, the scaffold demonstrates a proportional increase in run length as a function of attachment sites [Fig. 2(F)].

Finally, we demonstrate the power of this approach by patterning endogenously expressed protein complex from cellular lysate onto our DNA nanostructures. We took advantage of the *Saccharomyces cerevisiae* yeast GFP clone collection generated by Huh *et al*.[19] Huh *et al*. used homologous recombination to create a collection of strains expressing full-length, chromosomally-tagged GFP fusion proteins. We selected two strains expressing GFP-tagged subunits of the Arp2/3 complex, ArpC3 and ArpC4 (Fig. 3). The Arp2/3 complex is a stable seven-component protein complex that plays a crucial role in regulating the cellular actin network.[20] As illustrated in Figure 3(A), we used nanobody-labeled DNA nanostructures to pull out the GFP-tagged subunit from yeast lysate and then assessed the presence of Arp2 by Western blotting. For both GFP-tagged ArpC3 and ArpC4, the amount of Arp2 scales with the number of nanobody proteins on the nanostructures [Fig. 3(B,C)].

Discussion

Overall, this study establishes the broad utility of nanobody-based attachment to control protein labeling of DNA nanostructures. As fluorescently tagged proteins are widely available in both cell lines and animal models, this system demonstrates a simple approach for precisely patterning endogenous protein complexes straight from cellular lysates on to DNA nanostructures. As with co-immunoprecipitation experiments, these pull-downs do not require large amounts of starting material (≤10 μg/mL). Unlike co-immunoprecipitation, however, this technique enables one to label DNA nanostructures with precisely controlled geometry and stoichiometry. Besides demonstrating the feasibility of this technical advance for GFP-tagged proteins, it can easily be expanded to other nanobody- or monobody-based attachment systems.[13,21] Overall, this approach will expand the utility of DNA nanostructures to biological questions, such as the impact of microdomains on protein behavior and function.[22,23]

Materials and Methods

Nanobody–SNAP preparation

The DNA sequence for the GFP-nanobody was generated and synthesized by Genewiz off of the previously published "enhancer" GFP-nanobody sequence.[14,15] The SNAP-tagged nanobody construct contained from N- to C-terminus: the GFP-nanobody, a flexible $(Gly\text{-}Ser\text{-}Gly)_2$ linker, the SNAP-tag for oligo labeling, and both FLAG and 6xHis purification tags. Protein was expressed in Sf9 cells by transient transfection (pBiex-1; Escort IV, Sigma), and affinity purified at 72 h using anti-FLAG M2 affinity resin (Sigma) similar to previously published protocols.[16] Nanobody bound to anti-FLAG resin was incubated with excess (>10 μ*M*) BG-oligo-Cy3 in wash buffer (20 m*M* imidazole, 150 m*M* KCl, 5 m*M* $MgCl_2$, 1 m*M* EDTA, 1 m*M* EGTA, 1 m*M* DTT, 1 μg/mL PMSF, 10 μg/mL aprotinin, 10 μg/mL leupeptin, pH 7.4) at 37°C for 30 min followed by overnight incubation at 4°C, with continuous mixing during both steps.[4] Labeled-nanobody bound to resin was washed with wash buffer and eluted using 0.2 mg/mL FLAG peptide (Sigma). Protein labeling was confirmed by a 10% SDS gel followed by Coomassie

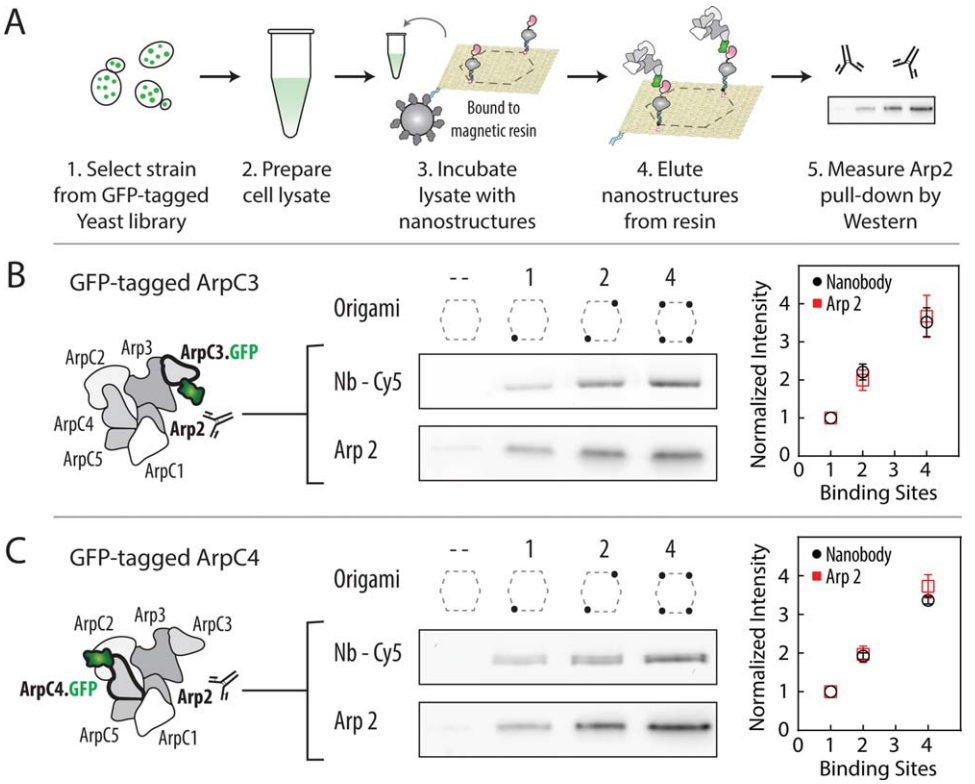

Figure 3. Patterning the Arp2/3 protein complex on DNA nanostructures. (A) Schematic of Arp 2/3 experimental protocol. Yeast lysate was prepared from (B) ArpC3-GFP, and (C) ArpC4-GFP expressing strains selected from the GFP-tagged yeast strain library.[19] Lysate was incubated with nanobody-labeled nanostructures bound to magnetic resin, eluted, and assessed by Western blotting for the Arp2 subunit. (B, C) Representative images are shown of Cy5 nanobody intensity and corresponding Arp2 Western band intensity for both ArpC3 and ArpC4 pulldowns. For both (B) ArpC3-GFP and (C) ArpC4-GFP, Arp2 scales with the number of nanobody on DNA nanostructures. Error bars are ± SEM ($n > 5$).

staining and Cy3-imaging with a Typhoon gel imager (GE Healthcare). The protein was stored in 55% glycerol (v/v) at −20°C.

Benzyl-guanine-labeled oligonucleotide preparation

Briefly, 0.17 m*M* C6-amine-oligo5-Cy3 (Supporting Information Table S1) was incubated with 11.6 m*M* benzyl-guanine NHS ester (NEB) for 4 h at 37°C with shaking at ≥1000 rpm. Labeled oligo was then purified twice into 2 m*M* Tris, pH 8.5 using Illustra ProbQuant G-50 micro columns (GE Healthcare).[4] Oligo concentration was determined from Cy3 intensity using a NanoDrop spectrophotometer.

Adenylyl cyclase and myosin VI preparation

Adenylyl cyclase constructs were based off of a previously published study.[16] Briefly, the cytoplasmic domains from isoform II and V (C2, isoform II; C1a, isoform V) were joined by a 30 nm linker, and fused with eGFP and a FLAG purification tag at the C-terminus. Adenylyl cyclase was expressed in Sf9 cells, purified as previously described, and used within 2 days of purification for maximal activity.[16] Myosin VI constructs contain from N- to C-terminus: residues 1–992 of *Sus scrofa* myosin VI (containing both the IQ and SAH domains), a leucine zipper for dimerization [GCN4],[24] eGFP, and a FLAG purification tag. Myosin VI was purified similar to previously described methods and stored in 55% glycerol (v/v) at −20°C.[4]

Scaffold labeling and preparation

Cy5-labeled DNA nanostructures were prepared based on the detailed description in previous work from our lab.[3,4] Briefly, a list of strand sequences is provided in Supporting Information Table S1. Each scaffold contains 23 Cy5 molecules for imaging and a biotinylated strand to facilitate purification of nanostructures. For formation of nanostructures, single-stranded M13mp18 DNA (NEB) was mixed with excess of short staple strands (IDT) in TAE–Mg^{2+} buffer (40 m*M* Tris, 20 m*M* acetic acid, 1 m*M* EDTA, 12.5 m*M* $MgCl_2$) followed by the annealing protocol listed in Supporting Information Table S2. For nanobody-labeling, Cy5-nanostructures were incubated for 10–15 min with streptavidin-coated magnetic beads (NEB) at 30°C with shaking in the appropriate reaction buffer containing 1 mg/mL BSA and 5–10 n*M* of a mixture of 42-nucleotide oligos with randomized sequences (blocking oligos). Resin was washed three times and then incubated with

excess Cy3-labeled nanobody for 10–15 min at 30°C with shaking.

Adenylyl cyclase activity

Five- to ten-fold excess adenylyl cyclase was incubated with nanobody-labeled nanostructures bound to magnetic resin for 10 min at 30°C with shaking in AC buffer [50 m*M* HEPES pH 8.0, 5 m*M* $MgCl_2$, 50 m*M* NaCl, 1 m*M* DTT, 1 mg/mL BSA, and 5–10 n*M* 42-nucleotide mix]. Resin was washed three times with AC buffer, and then incubated at 30°C with shaking for 30 min in 50 μL AC buffer containing 100 μ*M* ATP and 100 μ*M* forskolin (Sigma). At the end of 30 min, the reaction solution was removed from resin, separated into two 25 μL aliquots, and mixed with Kinase–Glo Max luminescent assay mix (Promega). End-point luminescence was measured in white, 96-well plates using an M5e Spectramax spectrophotometer (Molecular Devices) and corrected for pyrophosphate inhibition. Magnetic resin was washed with AC buffer, eluted with excess elution strand for 10–15 min at 30°C, and run on a 0.67% agarose 0.1% SDS gel to correct for nanostructure concentration.

Myosin motility assay

GFP-tagged myosin VI was incubated with nanobody-labeled nanostructures bound to magnetic resin and eluted in AB buffer (AB; 25 m*M* imidazole pH 7.4, 25 m*M* KCl, 4 m*M* $MgCl_2$, 1 m*M* EGTA, 1 m*M* DTT, 1 mg/mL BSA, and 5–10 n*M* random 42-nucleotide DNA mix) with 1–2 μ*M* elution strand according to Ref. 4. Keratocytes were derived from scales of *Rocio octofasciata* (Jack Dempsey Cichlids) as previously described.[25] All protocols conform to the guidelines of the local animal care and use committee (IACUC). Extraction of actin networks, elution of myosin VI-labeled nanostructures, imaging of myosin-driven nanostructure movement, and trajectory analysis followed previously published methods.[3,4]

Yeast Arp2/3 complex binding

S. cerevisiae expressing GFP-tagged ArpC3 (YLR370C) and ArpC4 (YKL013C) in an ATCC 201388 background (strain BY4741; *MAT*a *his3Δ1 leu2Δ0 met15Δ0 ura3Δ0)* were selected from the Yeast GFP Clone Collection (Invitrogen).[19] Yeast were grown in SD/-His minimal media (Clontech) at 30°C, and lysed by repetitive liquid N_2 freezing and grinding in YB buffer (50 m*M* HEPES pH 7.5, 100 m*M* KCl, 1 m*M* EGTA, 3 m*M* $MgCl_2$, 1 m*M* DTT, 50 μg/mL PMSF, 5 μg/mL aprotinin, and 5 μg/mL leupeptin). Clarified lysate was incubated with nanobody-labeled nanostructures bound to magnetic resin for 1 h at 4°C. Resin was washed three times with YB.BN buffer (YB buffer + 1 mg/mL BSA, and 5–10 n*M* random nucleotide mix), and then incubated at 30°C with shaking for 10 min in 40 μL YB.BN buffer containing 1–2 μ*M* elution strand. Elute was run on a 10% SDS gel and scanned for nanobody fluorescence on a Typhoon gel imager (GE Healthcare) before being transferred similar to previous published protocols.[26] Primary goat anti-Arp2 antibody (SC-11969, Santa Cruz Biotechnology) was used at a concentration of 1:200 and mouse antigoat secondary antibody (Jackson ImmunoResearch Laboratories) at 1:20,000. Blots were developed using Immobilon Western chemiluminescent HRP substrate (Millipore) and an Odyssey FC imaging system (LI-COR).

Acknowledgments

The authors thank H. Yan for hosting the atomic force microscopy experiments.

REFERENCES

1. Derr ND, Goodman BS, Jungmann R, Leschziner AE, Shih WM, Reck-Peterson SL (2012) Tug-of-war in motor protein ensembles revealed with a programmable DNA origami scaffold. Science 338:662–665.
2. Hariadi RF, Cale M, Sivaramakrishnan S (2014) Myosin lever arm directs collective motion on cellular actin network. Proc Natl Acad Sci USA 111:4091–4096.
3. Hariadi RF, Sommese RF, Adhikari AS, Taylor RE, Sutton S, Spudich JA, Sivaramakrishnan S (2015) Mechanical coordination in motor ensembles revealed using engineered artificial myosin filaments. Nat Nanotechnol 10:696–700.
4. Hariadi RF, Sommese RF, Sivaramakrishnan S (2015) Tuning myosin-driven sorting on cellular actin networks. eLife 4:e05472.
5. Fu J, Liu M, Liu Y, Woodbury NW, Yan H (2012) Interenzyme substrate diffusion for an enzyme cascade organized on spatially addressable DNA nanostructures. J Am Chem Soc 134:5516–5519.
6. Fu J, Yang YR, Johnson-Buck A, Liu M, Liu Y, Walter NG, Woodbury NW, Yan H (2014) Multi-enzyme complexes on DNA scaffolds capable of substrate channeling with an artificial swinging arm. Nat Nanotechnol 9:531–536.
7. Mei Q, Wei X, Su F, Liu Y, Youngbull C, Johnson R, Lindsay S, Yan H, Meldrum D (2011) Stability of DNA origami nanoarrays in cell lysate. Nano Lett 11:1477–1482.
8. Rinker S, Ke Y, Liu Y, Chhabra R, Yan H (2008) Self-assembled DNA nanostructures for distance-dependent multivalent ligand–protein binding. Nat Nanotechnol 3:418–422.
9. Numajiri K, Yamazaki T, Kimura M, Kuzuya A, Komiyama M (2010) Discrete and active enzyme nanoarrays on DNA origami scaffolds purified by affinity tag separation. J Am Chem Soc 132:9937–9939.
10. Timm C, Niemeyer CM (2015) Assembly and purification of enzyme-functionalized DNA origami structures. Angew Chem Int Ed 54:6745–6750.
11. Stephanopoulos N, Liu M, Tong GJ, Li Z, Liu Y, Yan H, Francis MB (2010) Immobilization and one-dimensional arrangement of virus capsids with nanoscale precision using DNA origami. Nano Lett 10:2714–2720.
12. Sacca B, Meyer R, Erkelenz M, Kiko K, Arndt A, Schroeder H, Rabe KS, Niemeyer CM (2010) Orthogonal protein decoration of DNA origami. Angew Chem Int Ed 49:9378–9383.

13. Muyldermans S (2013) Nanobodies: natural single-domain antibodies. Annu Rev Biochem 82:775–797.
14. Kirchhofer A, Helma J, Schmidthals K, Frauer C, Cui S, Karcher A, Pellis M, Muyldermans S, Casas-Delucchi CS, Cardoso MC, Leonhardt H, Hopfner KP, Rothbauer U (2010) Modulation of protein properties in living cells using nanobodies. Nat Struct Mol Biol 17:133–138.
15. Kubala MH, Kovtun O, Alexandrov K, Collins BM (2010) Structural and thermodynamic analysis of the GFP:GFP–nanobody complex. Protein Sci 19:2389–2401.
16. Ritt M, Sivaramakrishnan S (2016) Correlation between activity and domain complementation in adenylyl cyclase demonstrated with a novel FRET sensor. Mol Pharmacol 89:407–412
17. Hanoune J, Defer N (2001) Regulation and role of adenylyl cyclase isoforms. Annu Rev Pharmacol Toxicol 41:145–174.
18. Buss F, Spudich G, Kendrick-Jones J (2004) Myosin VI: cellular functions and motor properties. Annu Rev Cell Dev Biol 20:649–676.
19. Huh WK, Falvo JV, Gerke LC, Carroll AS, Howson RW, Weissman JS, O'Shea EK (2003) Global analysis of protein localization in budding yeast. Nature 425:686–691.
20. Goley ED, Welch MD (2006) The ARP2/3 complex: an actin nucleator comes of age. Nat Rev Mol Cell Biol 7: 713–726.
21. Koide A, Bailey CW, Huang X, Koide S (1998) The fibronectin type III domain as a scaffold for novel binding proteins. J Mol Biol 284:1141–1151.
22. Engelman DM (2005) Membranes are more mosaic than fluid. Nature 438:578–580.
23. Rao M, Mayor S (2014) Active organization of membrane constituents in living cells. Curr Opin Cell Biol 29:126–132.
24. Trybus KM, Freyzon Y, Faust LZ, Sweeney HL (1997) Spare the rod, spoil the regulation: necessity for a myosin rod. Proc Natl Acad Sci USA 94:48–52.
25. Sivaramakrishnan S, Spudich JA (2009) Coupled myosin VI motors facilitate unidirectional movement on an F-actin network. J Cell Biol 187:53–60.
26. Swanson CJ, Ritt M, Wang W, Lang MJ, Narayan A, Tesmer JJ, Westfall M, Sivaramakrishnan S (2014) Conserved modular domains team up to latch-open active protein kinase Calpha. J Biol Chem 289:17812–17829.